PHYSICAL REVIEW B **87**, 121103(R) (2013)

Time-resolved resistive switching on manganite surfaces: Creep and $1/f^{\alpha}$ noise signatures indicate pinning of nanoscale domains

Jon-Olaf Krisponeit,* Christin Kalkert, Bernd Damaschke, Vasily Moshnyaga, and Konrad Samwer
I. Physikalisches Institut, Universität Göttingen, Friedrich-Hund-Platz 1, 37077 Göttingen, Germany.
(Received 18 April 2012; published 13 March 2013)

We performed time-resolved nanoscale studies on the resistive switching of perovskite manganite thin films by means of conductive atomic force microscopy. Creep and recovery features have been observed in the evolution of metallic domains via pulse-train experiments and current map sequences. Local $I(t)$ curves show $1/f^{\alpha}$ noise signatures during the switching process, a phenomenon which occurs in various physical processes consisting of discrete jumps of different sizes, such as the Barkhausen effect. Our results imply that the resistive switching falls into this universal class of effects with dynamics determined by the pinning and depinning of structural domain walls.

DOI: 10.1103/PhysRevB.87.121103 PACS number(s): 75.47.Lx, 72.70.+m, 73.40.−c, 73.50.−h

Electrically driven resistive switching is a widely spread phenomenon in transition-metal oxides like perovskite manganites.[1–5] In most cases, the underlying mechanism is far from being understood. Several explanations have been proposed, including Schottky barriers,[5] oxygen vacancy electromigration,[3] and structural transitions.[6,7] The last scenario might apply especially for manganites, where—even at room temperature—the electrical properties are strongly affected by electron-lattice correlations effects.

The experimental approach to characterize resistive switching effects usually employs macroscopic contacts. Nanoscale techniques, like conductive atomic force microscopy (C-AFM), recently gained in importance because they are able to depict inhomogeneities of the switching behavior and to monitor the growth of switched regions in space and time. Furthermore, the applicability of future nonvolatile data storage concepts crucially relies on the reproducibility of the desired switching on small length scales and hence cannot be judged by macroscopic measurements alone. For manganites, only a few C-AFM studies have been published yet.[7–10] They focused mainly on the characterization of the different resistive states by $I(V)$ curves and the spatial appearance of resistively changed surface regions. The huge potential of this method for studying long-time evolution by successive scanning and, even more, in time-resolved spectroscopic modes has not been exploited extensively.

In a previous paper, we have shown that the switching process consists of the creeplike growth of nanoscale metallic domains.[7] In this Rapid Communication, we report C-AFM results further supporting the hypothesis of a structural transition responsible for resistive switching in manganites. Pulse-train experiments and fast C-AFM scans reveal creep and recovery behavior. We demonstrate that individual metallic domains on the nanometer scale are metastable, which might give an explanation for the decay effects observed in macroscopic setups. Further, single $I(t)$ spectra exhibit switching processes occurring on a variety of time scales, where the underlying current trend is accompanied by $1/f^{\alpha}$-like signatures. Hence, the results indicate that the resistive switching effect joins the wide family of crackling phenomena.[11] This class comprises, for instance, earthquakes, the magnetic Barkhausen effect, and martensitic phase transitions, which proceed in steplike events of different sizes. Since such crackling phenomena are all dominated by pinning-depinning effects, the noise signature found here agrees with the assumption of a structural transition being involved in the still unsolved resistive switching mechanism.

The experiments were performed on $La_{1-x}A_xMnO_3$ (A = Ca, Sr; thicknesses d = 30–50 nm) films, epitaxially grown on MgO(100) substrates by metalorganic aerosol deposition.[12] Working under ambient conditions this technique allows oxygen-deficient deposition to be avoided. Although the stoichiometric oxygen content was not verified directly for the thin films, it is reflected by the lattice parameters and metal-to-insulator transition temperatures agreeing with those of bulk samples.

Moreover, according to x-ray diffraction, manganite films are stress-free on MgO.[12] The C-AFM setup consists of a commercial AFM under ultrahigh-vacuum conditions which runs in contact mode. Conductively (Ti/Pt) coated cantilevers are used to perform electric measurements simultaneously with recording of the topography. The dominant resistance contribution comes from the tip-to-sample contact (the grounded counterelectrode is a macroscopic clamping contact). Therefore, the strongest electric fields are applied in the direct vicinity of the tip and only here is the resistive switching induced and recorded. All electrical measurements were recorded by the integrated amplification system, having an upper current limit of 50 nA and time resolution of 20 μs.

The switching effect can be observed for various different manganite samples and is not very sensitive to bulk properties. Here, the samples were studied by C-AFM at room temperature, all having a highly insulating initial surface state. They show bipolar resistive switching with threshold voltages of at least about 3 V, where positive pulses at the tip generate the metallic state and negative pulses restore the insulating one.[7]

We first present results obtained by pulse-train experiments on a $La_{0.8}Ca_{0.2}MnO_3$ surface. While scanning an area of 1×1 μm^2 at 11×11 positions current spectra were taken. The applied voltage sequences are illustrated in Fig. 1(a): pulse trains, each consisting of several hundred positive voltage pulses of length τ_a, are used to increase the local conductivity. Two subsequent pulses are separated by a constant waiting time τ_b, in which, by a small positive voltage, a single current value is recorded. Hence, the $I(t)$ curves depict the accumulative

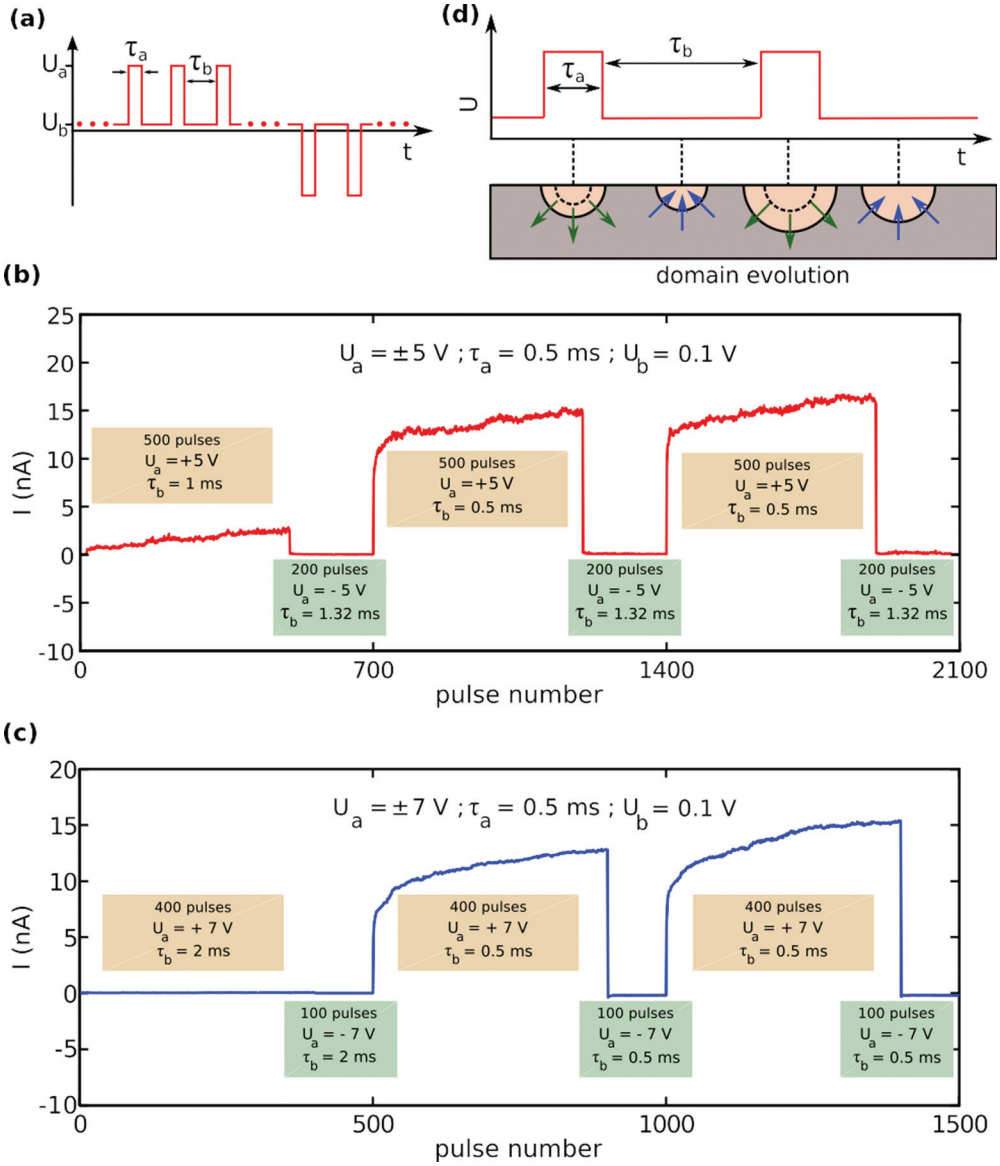

FIG. 1. (Color online) Pulse-train experiments on a $La_{0.8}Ca_{0.2}MnO_3$ thin film at room temperature. (a) The voltage sequence applied consists of of several trains of positive and negative pulses of duration τ_a and separated by the waiting time τ_b, in which only a small voltage is applied for current measurement. (b) A longer τ_b results in slower current increase, as shown in the first pulse train. (c) For even longer waiting times the current does not grow at all. (d) This behavior indicates that the metallic regions growing during the voltage pulse are shrinking during the waiting time.

effect of successive pulses and not the current evolution in between. Each experiment consists of three positive pulse trains. The pulse strength, duration, and number of pulses are identical for all three pulse trains, whereas the waiting time τ_b is varied. In between two positive series, shorter negative pulse trains were used to ensure a recreation of the insulating surface state.

In Fig. 1(b), a waiting time $\tau_b = 1$ ms was chosen for the first positive pulse train. Afterwards, two trains with a shorter waiting time, $\tau_b = 0.5$ ms, followed. The current evolution shown in Fig. 1(b) was averaged over 57 local spectra, where the maximum current exceeded a minimal value of 2 nA, i.e., where a switching event has been induced successfully. Being crucial for the generation of strong local electric fields, even small variations in the C-AFM tip-to-sample contact can avoid induction of resistive switching. During each pulse train, the current increases with the number of positive pulses applied. This directly mirrors the growth of a metallic region under the tip. Interestingly, the prolonged waiting time τ_b in the first pulse train results in a slower increase in comparison with the following ones. Since the second and third pulse trains show almost identical behavior, their faster increase cannot be attributed to training effects but must be regarded as a consequence of the shorter waiting time. Similar results are shown in Fig. 1(c); this time 21×21 spectra were taken and 94 considered as successful switching. Here, the waiting time of the first pulse train has been enlarged to $\tau_b = 2$ ms, which entirely suppresses the current growth. Again, shorter waiting

times in the second and third series produced the same current evolution as in Fig. 1(b).

On the assumption of a stable domain configuration after the positive pulse, these results cannot be understood. In each sequence, the overall pulse length is identical for all three pulse trains, and accumulation should consequently result in similar current evolutions. Instead, the measurements clearly show that the metallic state is metastable as it is more easily destroyed by negative pulses than it is created by positive ones. One could also assume a switching event induced directly at the tip under negative voltage, which disconnects the tip from the metallic domain. However, this scenario would include the formation of an additional—energetically unfavorable—interface. Furthermore, a recovery of the initially insulating surface state can indeed be observed even at the small positive measurement voltage during τ_b.

As we have shown previously, the metallic regions spread out in a creeplike manner during the voltage pulse.[7] Then the current behavior observed in the pulse-train experiments can be understood in a straightforward picture: Assuming a metallic domain growth at the contact region between the tip and the sample, the current increase is in direct correspondence to the achieved domain size. Assuming a structural transition, a mechanical stress builds up at the propagating interface between the generated metallic island and the surrounding insulating matrix. If the pinning forces are too small to stabilize the domain configuration after switching off the voltage, the insulating initial surface state is recovered.

We hence assume that the relaxation observed here is driven by strain and strong pinning centers are absent. Yet it is essentially a creeplike phenomenon and the relaxation time scale is expected to be governed by local influences, i.e., surface morphology, crystal defects, and large-scaled disorder effects. The hypothetic time evolution is illustrated in Fig. 1(d). In this qualitative model we assume an insulating surface layer where the switching is initiated. Since $La_{0.8}Ca_{0.2}MnO_3$ is orthorhombic, we here assume three-dimensional growth of pseudocubic metallic islands extending from the surface into the bulk. Note, however, that the vertical shape of the conducting domains and their structural symmetry cannot be depicted by C-AFM. The longer the waiting time between two successive pulses, the further the metallic island recovers towards its initially highly resistive state until the next positive voltage pulse is applied. The suppressed current increase in the first pulse train of Fig. 1(c) must be due to a full recovery during the waiting time, so that a subsequent pulse finds no remainder of the previously formed metallic domain.

In addition to the pulse-train studies given in Fig. 1, selected snapshots of a series of successively taken fast C-AFM scans from the same sample are shown in Fig. 2. Beforehand, under application of a single voltage pulse, $U = 5$ V for 10 ms, several metallic regions have been formed in the vicinity of the tip position. Whereas most regions recover quite fast, one object—highlighted by the light blue frame—survives for more than 30 min. The direct observation of this slow recovery process fits perfectly into the creep scenario sketched above.

Whereas other studies focused mainly on the remanent switching contribution, it has to be mentioned that Nian *et al.* reported a related decay phenomenon regarding both resistance states of $Pr_{0.7}Ca_{0.3}MnO_3$ samples on a comparable time scale

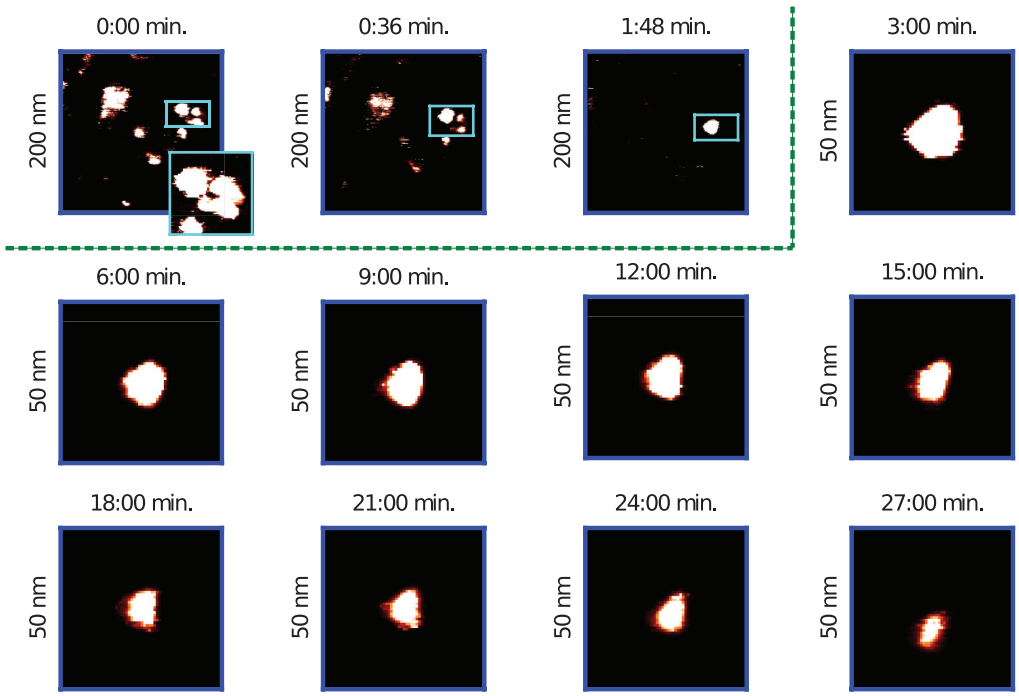

FIG. 2. (Color online) Recovery of the highly resistive state after a positive voltage pulse $U = 5$ V generated metallic domains on $La_{0.8}Ca_{0.2}MnO_3$ at room temperature. After the pulse, subsequent current maps have been taken rapidly. Most metallic regions disappear quickly; only the metallic object magnified in the first frame survives for longer than 2 min—it is highlighted in the first three frames. Afterwards, this region is magnified and shown for selected current maps; a slow recovery of the initially insulating surface is observed. The recovery process extended over more than 30 min.

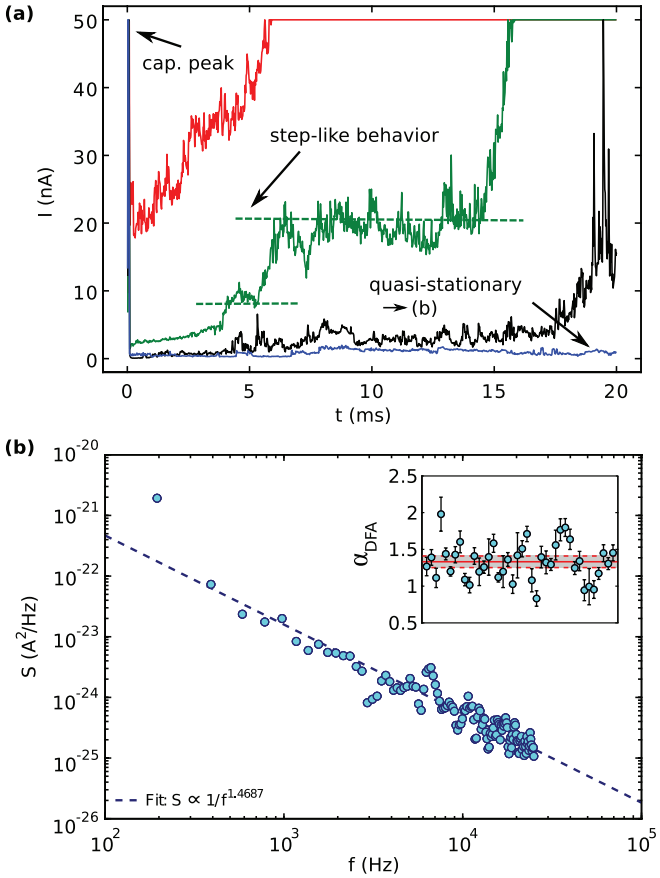

FIG. 3. (Color online) $I(t)$ spectra recorded during voltage pulses of $U = 7$ V on a $La_{0.8}Sr_{0.2}MnO_3$ surface at room temperature. (a) Four exemplary curves are shown, demonstrating the underlying switching to exhibit very different slopes. In addition, the curves show strong fluctuations. All curves start with a current peak presumably due to capacitive charging. Some $I(t)$ curves feature steplike current growth. (b) The power spectrum of the quasistationary blue $I(t)$ curve has been estimated by Welch's method. For nonstationary $I(t)$ curves, $1/f^{\alpha}$ behavior can be verified via DFA. The inset shows the obtained DFA results with error bars indicating the 95% confidence intervals of the DFA log-log fit. The horizontal lines mark the mean value, $\alpha = 1.33$, and its confidence region.

in the range of minutes.[13] While this was discussed in terms of oxygen vacancy diffusion, the structural explanation presented here agrees well with the observation of relaxation behavior in the magnetoresistive properties of $La_{0.7}Ca_{0.3}MnO_3$ also.[14]

We now finally address the question of how pinning effects influence the domain evolution. Therefore, in Fig. 3, we present $I(t)$ curves taken by C-AFM during 20-ms-long pulses of 7 V strength on a $La_{0.8}Sr_{0.2}MnO_3$ sample on 9×9 tip positions. The current increase during the switching process exhibits strongly varying velocities. The range spans from $I(t)$ curves reaching the instrumental saturation too fast to be resolved in detail down to curves showing no switching at all in the recorded time interval. In addition, the very first data points of all curves have a sharp current peak in common, which most probably corresponds to a capacitive charging of the sample. Note that the insulating surface layer sandwiched between the less resistive manganite bulk and the metallic tip resembles a capacitor.

Here, only 40 switching curves with intermediate slopes are to be examined, i.e., spectra where the current increase was resolvable by our experimental setup. Some of these are given in Fig. 3(a) as an example, illustrating the current increases with strongly varying slopes. In addition to the underlying switching trend, most curves show strong fluctuations which are far above the noise level of the instrument (several 10 pA). Further, steplike features can be seen in some $I(t)$ curves: the current stays for some time almost on a constant level before it increases in a sudden burst.

By switching over from the time to the frequency domain, more information about the switching dynamics can be revealed. In Fig. 3(b) the power spectral density S, as estimated by Welch's method,[15] is plotted against the frequency f. This exemplary spectrum was taken from the quasistationary blue $I(t)$ curve in Fig. 3(a) and suggests $S \propto 1/f^{\alpha}$ noise, here with a scaling exponent $\alpha \approx 1.5$. Whereas this selected curve can be regarded as quasistationary, i.e., having a mean value not changing significantly in time, all switching curves are intrinsically nonstationary, of course.

For such noise which occurs in addition to the switching trend, Welch's method is not applicable. We here employed detrended fluctuation analysis[16,17] (DFA) and estimated the DFA scaling exponent h, a generalized Hurst exponent. Therefore, after discarding the capacitive peak, we extracted a segment of the spectra ranging from the first value exceeding a lower limit of 0.2 nA—which is far above the instrument noise level—to the first value reaching the instrumental saturation limit of 50 nA. Furthermore, the $I(t)$ curves have been truncated to a small amount in order to increase the number of DFA divisors. Applying this technique all 40 curves, we can average the DFA scaling exponent to $h = 1.17 \pm 0.04$ on a confidence level of 95%. The scaling exponent h determined by the DFA algorithm can be directly converted to a scaling exponent $\alpha = 2h - 1 = 1.34 \pm 0.08$ characterizing the power-law behavior of the spectral density, $S \propto 1/f^{\alpha}$. The inset of Fig. 3(b) shows the rather large scattering of the individually determined scaling exponents α around the mean value. The error bars visualize 95% confidence intervals of the DFA log-log fit.

Considering that the time series is rather short and the method is locally sensitive, such strong scattering of the scaling exponents has to be expected. Whereas far more extensive studies would be necessary for a precise determination of the characteristic scaling exponent h, or α respectively, for the vast majority of spectra $\alpha = 1, \ldots, 2$ holds. Furthermore, application of Welch's method on the same $I(t)$ curve segments yields $\alpha = 1.35 \pm 0.05$, demonstrating that in our case the $1/f^{\alpha}$ noise signatures are actually dominant in comparison with the overall switching trend. In conclusion, the scaling exponents, the sometimes steplike form of the $I(t)$ curves, and the spectral density of the selected quasistationary process depicted in Fig. 3(b) all indicate that the switching process is accompanied by a crackling noise phenomenon.

It has been shown for a large variety of physical systems that such $1/f^{\alpha}$ crackling noise corresponds to transitions consisting of abrupt, avalanchelike events of different sizes.[11] In solid state physics, for instance, Barkhausen jumps in ferromagnets[18] as well as the conductivity during martensitic structural transitions[19,20] exhibit crackling noise with similar

exponents in the power spectral density. Recently Barkhausen noise has been found in the ferroelastic response of the distorted perovskite $LaAlO_3$.[21]

Although, in our case, the microscopic processes cannot be reconstructed from the type of switching noise observed, the similar scaling behavior of the power spectrum strongly suggests an analogous transition taking place, formed by many spontaneous bursts of varying size. The most natural scenario to explain such an avalanchelike switching behavior is indeed that of a structural transition whose dynamics is controlled by strong pinning forces. Assuming a structural switching process, creep phenomena and crackling noise could be understood in direct analogy to magnetic creep and Barkhausen noise. In Fig. 3, the fluctuation strength increases with the current growth. This observation cannot be attributed to local heating,[7] but inhomogeneities in the metallic domains (as indicated in the first frame of Fig. 2), their specific shape, and percolative effects might give an explanation.

In summary, C-AFM pulse-train measurements as well as fast scanned current maps indicate creep and recovery features in the domain growth of metallic islands during the resistive switching of manganite surfaces. DFA analysis of $I(t)$ switching curves gave an estimate for a scaling exponent $\alpha \approx 1.3$ for the power spectral density $S = 1/f^{\alpha}$. This noise signature indicates that the resistive switching process falls into the large class of crackling effects and agrees well with the hypothesis of a structural transition as key feature of the mechanism.

In terms of technological applicability our results point out nanoscale recovery processes as a major obstacle for nonvolatile memory concepts. However, a solution might be found in the control of pinning center densities.

We thank S. Hühn for sample preparation. M. Michelmann and M. Jungbauer have contributed to this work by helpful discussions. Financial support by DFG via SFB 602, A2, and the Leibniz program is acknowledged.

*jkrispo@gwdg.de

[1] A. Sawa, Mater. Today **11**, 28 (2008).
[2] A. Beck, J. G. Bednorz, C. Gerber, C. Rossel, and D. Widmer, Appl. Phys. Lett. **77**, 139 (2000).
[3] A. Baikalov, Y. Q. Wang, B. Shen, B. Lorenz, S. Tsui, Y. Y. Sun, Y. Y. Xue, and C. W. Chu, Appl. Phys. Lett. **83**, 957 (2003).
[4] S. Q. Liu, N. J. Wu, and A. Ignatiev, Appl. Phys. Lett. **76**, 2749 (2000).
[5] A. Sawa, T. Fujii, M. Kawasaki, and Y. Tokura, Appl. Phys. Lett. **85**, 4073 (2004).
[6] C. Jooss, J. Hoffmann, J. Fladerer, M. Ehrhardt, T. Beetz, L. Wu, and Y. Zhu, Phys. Rev. B **77**, 132409 (2008).
[7] J.-O. Krisponeit, C. Kalkert, B. Damaschke, V. Moshnyaga, and K. Samwer, Phys. Rev. B **82**, 144440 (2010).
[8] X. Chen, N. Wu, J. Strozier, and A. Ignatiev, Appl. Phys. Lett. **89**, 063507 (2006).
[9] C. Kalkert, J.-O. Krisponeit, M. Esseling, O. I. Lebedev, V. Moshnyaga, B. Damaschke, G. van Tendeloo, and K. Samwer, Appl. Phys. Lett. **99**, 132512 (2011).
[10] C. Moreno, C. Munuera, S. Valencia, F. Kronast, X. Obradors, and C. Ocal, Nano Lett. **10**, 3828 (2010).
[11] J. P. Sethna, K. A. Dahmen, and C. R. Myers, Nature (London) **410**, 242 (2001).
[12] V. Moshnyaga, L. Sudheendra, O. I. Lebedev, S. A. Köster, K. Gehrke, O. Shapoval, A. Belenchuk, B. Damaschke, G. van Tendeloo, and K. Samwer, Phys. Rev. Lett. **97**, 107205 (2006).
[13] Y. B. Nian, J. Strozier, N. J. Wu, X. Chen, and A. Ignatiev, Phys. Rev. Lett. **98**, 146403 (2007).
[14] R. von Helmolt, J. Wecker, T. Lorenz, and K. Samwer, Appl. Phys. Lett. **67**, 2093 (1995).
[15] P. D. Welch, IEEE Trans. Audio Electroacoust. **15**, 70 (1967).
[16] C.-K. Peng, S. V. Buldyrev, S. Havlin, M. Simons, H. E. Stanley, and A. L. Goldberger, Phys. Rev. E **49**, 1685 (1994).
[17] R. Weron, Physica A **312**, 285 (2002).
[18] P. J. Cote and L. V. Meisel, Phys. Rev. Lett. **67**, 1334 (1991).
[19] J. Ortín, I. Ràfols, L. Carrillo, J. Goicoechea, E. Vives, L. Mañosa, and A. Planes, J. Phys. IV **5**, C8-209 (1995).
[20] U. Chandni, A. Ghosh, H. S. Vijaya, and S. Mohan, Phys. Rev. Lett. **102**, 025701 (2009).
[21] R. J. Harrison and E. K. H. Salje, Appl. Phys. Lett. **97**, 021907 (2010).